Jelena POPOVIĆ CUKOVIC, Beno KLOPČIČ, Drago DOLINAR

University of Maribor, Faculty of Electrical Engineering and Computer Science

Analysis of stator winding tester for AC machines

Abstract. This paper describes a tester, which is developed to detect the right connection of the stator coils and direction of field rotation. The tester detects the magnetic flux density distribution in the air gap. Stator coils of synchronous machine (SM) without rotor are supplied by three-phase sinusoidal voltages. The corresponding magnetic field distribution is measured by analogue or bipolar digital Hall probes mounted on printed circuit board, which are placed near to each stator tooth. The proposed principle of testing has been proven with numerical analysis (FEM), analytical equations and experiment.

Streszczenie. W artykule opisano tester dla detekcji prawidłowości połączenia uzwojenia stojana i kierunku wirowania pola. Tester bada rozkład indukcji magnetycznej w szczelinie powietrznej. Cewki stojana silnika synchronicznego zasila się, przy usuniętym wirniku, trójfazowym napięciem sinusoidalnym i dokonuje pomiaru indukcji magnetycznej czujnikami Halla. Idea tego testu została potwierdzona przez symulację numeryczną (MES), rozwiązania analityczne i doświadczenie. (Analiza testera uzwojenia stojana maszyn prądu zmiennego).

Keywords: electromagnetic field, finite element method, Hall probes, stator winding.
Słowa kluczowe:.pole elektromagnetyczne, metoda elementów skończonych, czujnik Halla, uzwojenie stojana.

Introduction

The right connected coils of stator winding are basic precondition for the correct working of electrical machines. Fault detection in stator windings is attractive topics nowadays [1,2]. The authors in all cited papers deal with analysis and detection of faults, which can occur during the use of machine under normal conditions. The main goal is to follow the stator winding over the on-line system. On-line system used for checking stator windings is more common and often described in the literature. However, there are no reports in the literature on testing procedures of stator windings in the manufacturing process. The exception is [3], where the simple stator winding tester (SWT) is developed. The tester is based on magnetic field density measurements using only two Hall probes. However, it is confirmed that the tester has a number of disadvantages, which are entirely fixed by the modified and upgraded SWT described here. This paper presents the SWT, which detects either a wrong connection of coils or incorrect number of turns. This tester contains the same number of magnetic field sensors and stator teeth, which is different as it is described in [3] and it is appropriate testing device for all rotational and linear electric machines as well as for induction and synchronous electric machines.

The tester is based on the analysis of the magnetic field in air gap without rotor. Three-phase stator winding is supplied by symmetrical three-phase source of frequency 50 Hz. Harmonic excitation causes time dependent magnetic field that can be easily measured with Hall probes, which convert the measured magnetic field into Hall voltage. The analysis of SWT is conducted with analogue Hall probes, while the industrial realization of tester contains bipolar digital Hall probes, because digital signals are easier for further processing. However, in both cases, Hall probes are mounted at the printed circuit board and are placed close to the each stator tooth (see Figs. 1 and 5). The output voltages of each Hall probe in the case of corresponding balanced three-phase sinusoidal excitation of stator windings are for the certain angle shifted sinusoidal functions (or step-vice changing functions in case of a bipolar digital Hall probes). The sum of these angles around the stator is equal to $2p\pi$, where p is the number of pole pairs and it is one of the two testing conditions for the correct winding connection. The direction of the magnetic field is determined on the basis of time delay between Hall voltages of two probes mounted on two successive stator teeth. The previously developed generation of SWT [3] is not easily applicable, because it is awkward to shift Hall probes manually along each pair of stator teeth. Moreover, besides being very time-consuming, it is sometimes impossible to apply it for machines with small rotor diameter. Working of the SWT is verified in three different ways. Second section describes the finite element (FE) model of the tester. FEM based analysis calculates the flux linkages in the air gap. These flux linkages are given in the complex form as phasors by their magnitudes and angles. Afterwards, the angles between 12 calculated or measured phasors of flux linkages are calculated. The sum of calculated angles must be quite close to the ideal value $2p\pi$ for correct winding connection. The third section contains the analytical approach, based on the analysis of the stator equivalent circuit. Measured Hall voltages on stator with probes without any faults are given in the fourth section, as well as the comparison of the results. Section five describes the experimental findings due to some faults that frequently occur in the stator winding. It is succeeded by the conclusion.

FE model of analyzed SM

The tested synchronous motor (SM) is shown in Fig. 1. The stator has z=12 teeth, the winding is connected in such way that the number of poles equals $2p$=10. Therefore, the sum of 12 angles between the calculated phasors of coil flux linkages must be approximately 10π rad. However, the variations between 9.8π rad and 10.2π rad are allowed to recognize the stator winding connection as correct. Each angle must be between 0.69π rad and 0.96π rad that refers to the minimal and maximal angle. These values are different for each type of the electrical machine.
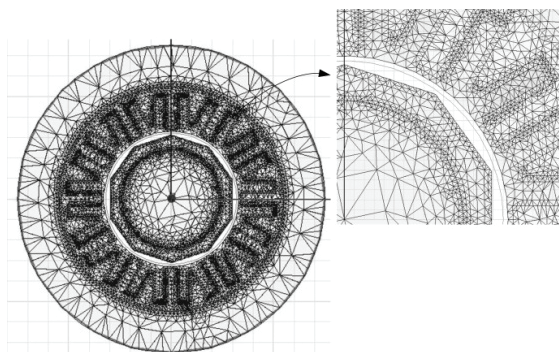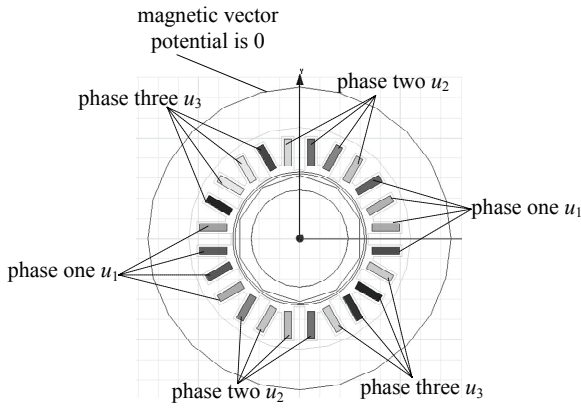

Fig.1. FE meshed model of SM

Fig.2. Geometry of analyzed SM with boundary conditions

The coils are supplied by symmetrical three-phase voltages of frequency 50 Hz. Each phase consists of four coils. When testing with SWT, there is no rotor in tester, therefore, FE model contains a rotor made of air. The Dirichlet boundary condition is set around the stator yoke (see Fig. 2). The FEM solver calculates the magnetic flux on the basis of the magnetic flux density and the corresponding area [4]. Remember that the magnetic vector potential, $\mathbf{A}$, is defined to be a field that satisfies the equation (1):

$$(1) \qquad \mathbf{B} = \nabla \times \mathbf{A}$$

where $\mathbf{B}$ is magnetic field density. The magnetic vector potential, $\mathbf{A}$, is set to a constant value on a boundary. Normally, this type of boundary condition is used to specify the potential of outer boundaries. It can also be used to set the interface between two objects to a potential, modelling the presence of a very thin conductor between the objects. In general, the magnetic field is tangential to any boundary on which magnetic vector potential is set to a constant. If the potential is a function of position, the partial derivatives of $\mathbf{A}$ with respect to coordinates are not necessarily zero. It all depends on what type of math function is used to specify the potential. Thus, $\mathbf{B}$ may not be tangential to the boundary and some flux will cross it. When time and position distribution of $\mathbf{B}$ for all 12 stator coils is determined, flux linkage Ψ can be obtained by applying Gauss law [5]. Magnetic flux linkage is time and position dependant as well, and it can be represented in a complex form by a vector called phasors [6]. Each of 12 flux linkages are therefore given with a magnitude and phase that can be written by (2):

$$(2) \qquad \mathbf{\psi}_i = |\psi_i| \cdot e^{j\phi_i} \cdot e^{j\omega t}, \; i = 1,2,3...12 \,.$$

Circuit model of the analyzed synchronous machine

The stator of the tested SM can be represented with the circuit model shown in Fig. 3. Each stator coil i is represented with ohmic resistance R_i, self inductance L_i and mutual inductance M_{ij} between coil i and j. The stator contains 12 coils, and all necessary coil data are given in Table I. Mutual inductances between two successive coils are equal and the influence between stator coils shifted for the same number of coils is also equal. Additionally, mutual inductances fulfil condition (3):

$$(3) \quad M_{ij} = M_{ji}, \quad i = 1,2,3...12, \quad j = 1,2,3...12, \, i \neq j \,.$$

When the stator windings are supplied with a symmetrical three-phase sinusoidal voltage, the time and position dependant magnetic field is excited. The obtained flux linkages can be also expressed in complex form by phasors introduced by (2). Note that Fig. 3 is an illustrative equivalent circuit and it does not show the real stator geometry. The stator coils are placed in a circle, which means that the stator coils are close enough to each other to ensure the mutual inductance between each and every one of them. The voltage balance of circuit model in Fig. 3 is given by (4):

$$(4) \qquad \mathbf{U} = \mathbf{Z} \cdot \mathbf{I}$$

where $\mathbf{U} = [u_1 \; u_2 \; u_3]^\mathsf{T}$ is the voltage matrix, $\mathbf{Z}$ is the so-called impedance matrix and $\mathbf{I} = [\,i_1 \; i_2 \; i_3\,]^\mathsf{T}$ is a current matrix. The current $\mathbf{I}$ is calculated from (4) with (5):

$$(5) \qquad \mathbf{I} = \mathbf{Z}^{-1}\mathbf{U}$$

where $\mathbf{Z}^{-1}$ is the inverse of the impedance matrix $\mathbf{Z}$. Determination of $\mathbf{I}$ and corresponding flux linkages is explained in the Appendix. Note that the complex notation in Appendix is used in order to easily calculate angles between the phasors.

Table I. Measured parameters of stator coils

Quantity	Unit	Value
number of turns N		300
wire diameter	mm	0.5
specific conductivity	S/m	$58 \cdot 10^6$
self-inductance L	mH	13.7
mutual inductance M_{12}*	mH	0.95
mutual inductance M_{13}*	mH	0.364
mutual inductance M_{14}	mH	0.114
mutual inductance M_{15}	mH	0.031
mutual inductance M_{16}	mH	0.038
mutual inductance M_{17}	mH	0.053
resistance R	Ω	4.2

*note that mutual inductance between two coils next to each other is denoted as M_{12} and it has the same value for each pair of coils; mutual inductance between every first and every third coil is denoted as M_{13}, and also has the same value for each pair of coils, etc.

Analysis of the results and presentation of industrial SWT

Analysis of all three presented methods is conducted with stator coils without any fault. Fig. 4 shows two flux linkages Ψ_1, Ψ_2 obtained with FEM for stator coil 1 and 2. Flux linkages of all 12 coils can be expressed with phasors and therefore, the angles ξ_i are easily calculated by (6):

$$(6) \quad \begin{aligned} e^{j\xi_i} &= \frac{\mathbf{\psi}_i}{\mathbf{\psi}_{i+1}} = \frac{|\psi_i| \cdot e^{j\phi_i} \cdot e^{j\omega t}}{|\psi_{i+1}| \cdot e^{j\phi_{i+1}} \cdot e^{j\omega t}} = \frac{e^{j\phi_i}}{e^{j\phi_{i+1}}} \\ &= e^{j(\phi_i - \phi_{i+1})}, \; \rightarrow \xi_i = \phi_i - \phi_{i+1}, i = 1,2,3...12. \end{aligned}$$
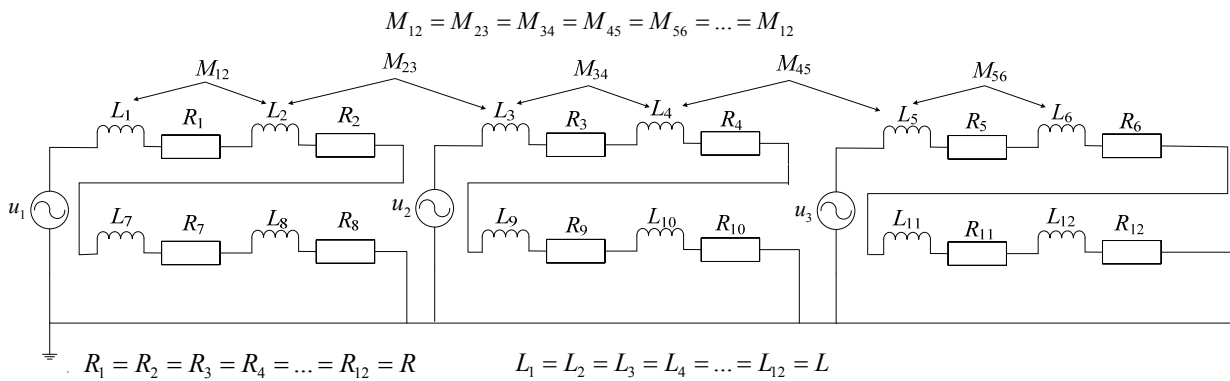
$$M_{12} = M_{23} = M_{34} = M_{45} = M_{56} = ... = M_{12}$$

Fig.3. Circuit model of analyzed stator windings

$$R_1 = R_2 = R_3 = R_4 = ... = R_{12} = R \qquad L_1 = L_2 = L_3 = L_4 = ... = L_{12} = L$$

Angles ξ_i calculated with FEM are given in table II. The sum of all corresponding angles is 9.936π and it is close to the theoretical value of $10\,\pi$. In other words, it is sufficient to check the time delay between corresponding magnetic fluxes, since that FE analysis enables the complete view time dependent view of quantities. Angles between magnetic flux linkages, which are obtained with the circuit approach are calculated in the same way using (6). The analytical results are also presented in Table II and sum of all angles is 9.93π and again, close to theoretical value of $10\,\pi$. Magnetic flux density is measured experimentally with Hall probes [7], which are placed on each stator tooth in the air gap (Fig. 6). Hall probe output is Hall voltage that is proportional to the flux density, which can be also interpreted as a phasor. Time delay between the two successive Hall voltages is proportional to the angle, which occurs between two corresponding flux linkage phasors. Figure 5 shows only two Hall voltages u_{Hall1} and u_{Hall2}. Angles obtained experimentally are given in Table II. The sum of all angles is, again, close to $10\,\pi$. It is necessary to emphasize that industrial application of SWT (Fig. 6) containing bipolar digital Hall probes. With such digital outputs, further signal processing is easier and faster. The output voltage from bipolar digital Hall probes is square wave, the time delays between the outputs from two successive probes represents angle, which is equivalent to that one measured with analogue Hall probes. As it is shown in Figs. 4 and 5, from the magnetic flux linkage waveforms and Hall voltages waveforms, flux linkage Ψ_2 and Hall voltage u_{Hall2} are lagged behind Ψ_1 respectively u_{Hall1}. Therefore, the magnetic field direction is mathematically positive. The other way around (flux linkage Ψ_1 and Hall voltage u_{Hall1} are lagged behind Ψ_2 respectively u_{Hall2}) means that the magnetic field direction is mathematically negative.

The comparison of the results obtained by FEM analysis, analytical calculation based on circuit approach and measurements obtained by the SWT shown in Fig. 6 is given in Tab. II. The agreement of the results is good. The sum of all angles determined by FEM and measurement equals 9.936π, while the sum of angles determined by a circuit approach equals $9.96\,\pi$, which is even closer to the theoretical value 10π. The determined values of angles also fulfil following the condition $0.69\pi < \xi_i < 0.96\pi$
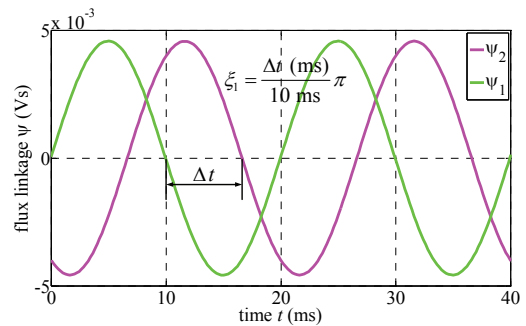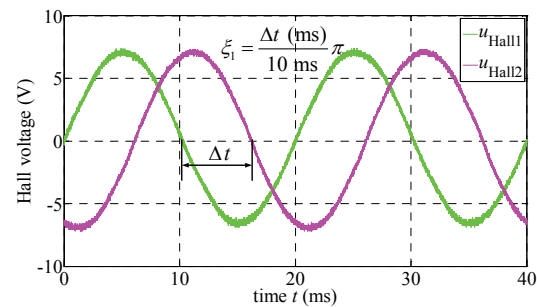

Fig. 4. Flux linkages calculated with FEM

Fig. 5. Hall voltages of the first and second probe obtained with analogue Hall probes

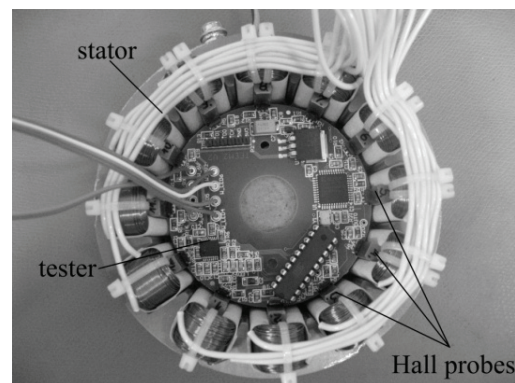Fig. 6. Industrial application of SWT

TABLE II. PHASE DIFFERENCE CALCULATED WITH FEM, MEASURED PHASE DIFFERENCE AND ANALYTICAL **CALCULATIONS**

	ξ_1/π	ξ_2/π	ξ_3/π	ξ_4/π	ξ_5/π	ξ_6/π	ξ_7/π	ξ_8/π	ξ_9/π	ξ_{10}/π	ξ_{11}/π	ξ_{12}/π	$\sum_{i=1}^{12}\xi_i/\pi$
FEM	0.723	0.933	0.723	0.933	0.723	0.933	0.723	0.933	0.723	0.933	0.723	0.933	9.936
Exper	0.76	0.9	0.75	0.89	0.76	0.91	0.75	0.9	0.76	0.9	0.75	0.9	9.93
Circuit	0.738	0.922	0.738	0.922	0.738	0.922	0.738	0.922	0.738	0.922	0.738	0.922	9.96

Conclusion

Checking of stator windings connection is a common measure of reliable manufacturers of AC machines. The basic operation principle of a simple stator winding tester shown in the paper is analyzed by FEM based numerical analysis of the magnetic field in the air gap and by analytical calculation based on circuit model of the analyzed stator. Both results agree very well with the measurements obtained by the industrial SWT. Rotation direction of magnetic field is determined from the time delay of voltages or magnetic fluxes obtained from two successive stator teeth.

Appendix

The analytical solution is based on circuit model of stator winding (Fig. 3). Each stator coil is represented with ohmic resistance and inductance and is magnetically coupled with all other stator coils. Consequently, there are seven different mutual inductances that are given in Table 1. The influence between the first and the sixth coil is equal to the mutual inductance between the first and the eight coil due to the rotational symmetry of the SWT (see Table I, $M_{16}=M_{18}$). The voltage balance is given by (4). The supply voltage is three-phase sinusoidal. Impedance matrix **Z** given by (7) is symmetrical because the stator is completely rotationally symmetrical:

$$(7) \quad \mathbf{Z} = \begin{bmatrix} z_{11} & z_{12} & z_{13} \\ z_{21} & z_{22} & z_{23} \\ z_{31} & z_{32} & z_{33} \end{bmatrix}$$

where

$$z_{11} = z_{22} = z_{33} =$$
$$4R + 4X_L e^{j\frac{\pi}{2}} + 4X_{12} e^{j\frac{\pi}{2}} - 4X_{16} e^{j\frac{\pi}{2}} + 4X_{17} e^{j\frac{\pi}{2}}$$
$$z_{12} = z_{21} = z_{13} = z_{31} = z_{23} = z_{32} =$$
$$\left(-2X_{12} + 4X_{13} - 4X_{15} + 2X_{16}\right) e^{j\frac{\pi}{2}}$$

and

$$X_L = \omega L, \; X_{12} = \omega M_{12}, \; X_{13} = \omega M_{13}, \; X_{14} = \omega M_{14},$$
$$X_{15} = \omega M_{15}, \; X_{16} = \omega M_{16}, \; X_{17} = \omega M_{17}.$$

Currents are calculated from (5). Once the currents are determined, the magnetic flux linkages are calculated by (8):

$$\mathbf{\psi}_1 = \left|\psi_1\right| e^{j\phi_1} e^{j\omega t} = \left|I_1\right| e^{j\varphi_1} e^{j\omega t} \cdot$$
$$\left(j\omega L + j\omega M_{12} - j\omega M_{16} + j\omega M_{17}\right) +$$
$$(8) \quad + \left|I_2\right| e^{j\varphi_2} e^{j\omega t} \cdot \left(-j\omega M_{12} + j\omega M_{13} - j\omega M_{15} + j\omega M_{16}\right)$$
$$+ \left|I_3\right| e^{j\varphi_3} e^{j\omega t} \cdot \left(j\omega M_{13} - j\omega M_{14} - j\omega M_{15} + j\omega M_{14}\right),$$
$$\vdots$$

$$\mathbf{\psi}_{12} = \left|\psi_{12}\right| e^{j\phi_{12}} e^{j\omega t} = \dots.$$

Corresponding angles between flux linkages phasors ξ_i of all 12 coils are calculated by (6) and are given in Table II.

REFERENCES
[1] S. Nandi, H.A. Toliyat and X. Li: Condition monitoring and fault diagnosis of electric motors—a review, IEEE Trans. on energy conversion, vol.20, no. 4, pp. 719-129, Dec. 2005.
[2] H. Hemano, C. Demian and G.A. Capolino: A frequency-domain detection of stator winding faults in induction machines using an external flux sensor, IEEE trans. on industy application,vol. 39, no.5, pp. 1272-1279, Sept. 2003.
[3] Patent application website: http://publikationen.dpma.de, patent application number: DE102006050551(A1), B. Klopcic @ Robert Bosch GmbH.
[4] Programme tool Maxwell 12, Ansoft, 2008.
[5] J. A. Stratton: *Electromagnetic Theory*, John Wiley & Sons, Inc., Hoboken, New York, 2007.
[6] K. Sahay and S. Pathak: *Basic concepts of electrical engineering*, NEW AGE INTERNATIONAL (P) LIMITED, PUBLISHERS, 4835/24, Ansari Road, Daryaganj, New Delhi, India, 2006.
[7] Manuals for analogue Hall probes: model 91SS12-2

Authors: Jelena Popović Cukovic, B.Sc. Electrical engineering, junior researcher, Faculty of Electrical Engineering and Computer Science, Smetanova 17, 2000 Maribor, Slovenia E-mail: jelena.popovic@uni-mb.si; dr. Beno Klopčič, PhD Electrical Engineering, senior researcher, Faculty of Electrical Engineering and Computer Science, Smetanova 17, 2000 Maribor; prof. dr. Drago Dolinar, PhD Electrical Engineering, Faculty of Electrical Engineering and Computer Science, Smetanova 17, 2000 Maribor, Slovenia E-mail: dolinar@uni-mb.si;